Korean J. Chem. Eng., **17**(1), 86-92 (2000)

Characterization of Tungsten Oxide Supported on TiO_2 and Activity for Acid Catalysis

Jong Rack Sohn† and Jung Hoon Bae

Department of Industrial Chemistry, Engineering College, Kyungpook National University, Taegu 702-701, Korea

(Received 29 September 1999 • accepted 13 November 1999)

Abstract−Tungsten oxide-titania catalysts were prepared by drying powdered $Ti(OH)_4$ with ammonium metatungstate aqueous solution, followed by calcining in air at high temperature. Characterization of prepared catalysts was performed by using FTIR, Raman, XPS, XRD, and DSC and by measuring surface area. Upon the addition of tungsten oxide to titania up to 20 wt%, the specific surface area and acidity of catalysts increased in proportion to the tungsten oxide content due to the interaction between tungsten oxide and titania. Since the TiO_2 stabilizes the tungsten oxide species, for the samples equal to or less than 20 wt%, tungsten oxide was well dispersed on the surface of titania, but for the samples containing 25 wt% or above 25 wt%, the triclinic phase of WO_3 was observed at calcination temperature above 400 °C. The catalytic activities for 2-propanol dehydration and cumene dealkylation were correlated with the acidity of catalysts measured by ammonia chemisorption method.

Key words: WO_3/TiO_2 Catalyst, Characterization, Acid Catalysis, 2-Propanol Dehydration, Cumene Dealkylation

INTRODUCTION

Solid acid catalysts play an important role in hydrocarbon conversion reactions in the chemical and petroleum industries [Cheung et al., 1995; Tanabe et al., 1989; Lee and Rhee, 1997]. Many kinds of solid acids have been found; their acidic properties on catalyst surfaces, their catalytic action, and the structure of acid sites have been elucidated for a long time, and those results have been reviewed by Arata [Arata, 1990]. The strong acidity of zirconia-supported sulfate attracted much attention because of its ability to catalyze many reactions such as cracking, alkylation, and isomerization. The potential for a heterogeneous catalyst has yielded many papers on the catalytic activity of sulfated zirconia materials [Arata, 1990; Keogh et al., 1995; Figueras et al., 1997]. Sulfated zirconia incorporating Fe and Mn has been shown to be highly active for butane isomerization, catalyzing the reaction even at room temperature [Hsu et al., 1992; Adeeva et al., 1995].

Several workers have reported that the addition of platinum to zirconia modified by sulfate ions enhances catalytic activity in the skeletal isomerization of alkanes without deactivation when the reaction is carried out in the presence of hydrogen [Ebitani et al., 1991; Vaudagna et al., 1997]. The high catalytic activity and small deactivation can be explained by both the elimination of the coke by hydrogenation and hydrogenolysis and the formation of Brönsted acid sites from H_2 on the catalysts [Ebitani et al., 1991]. Recently, Hino and Arata reported zirconia-supported tungsten oxide as an alternative material in reaction requiring strong acid sites [Arata, 1990; Hino and Arata, 1987]. Several advantages of tungstate, over sulfate, as dopant include that it does not suffer from dopant loss during thermal treatment and it undergoes significantly less deactivation during catalytic reaction. So far, however, supported tungsten oxide catalysts have been mainly on alumina and silica [Basrur et al., 1991; Meijers et al., 1995], and only some work has been studied for the TiO_2 support. Moreover, there is no systematic study using a variety of instruments, although some limited work by Infrared spectroscopy and X-ray diffraction was reported [Gutierrez-Alejandre et al., 1998; Alemany et al., 1996].

This paper describes the characterization of tungsten oxide supported on titania and catalytic activity for acid catalysis. The characterization of the samples was performed by means of Fourier transform infrared (FTIR), X-ray diffraction (XRD), X-ray photoelectron spectroscopy (XPS), Raman, Differential scanning calorimetry (DSC), and by the measurement of surface area.

EXPERIMENTAL

The precipitate of $Ti(OH)_4$ was obtained by adding aqueous ammonia slowly into a mixed aqueous solution of titanium tetrachloride and hydrochloric acid at room temperature with stirring until the pH of aqueous solution reached about 8. The precipitate thus obtained was washed thoroughly with distilled water until chloride ion was not detected by $AgNO_3$ solution, and was dried at room temperature for 12 h. The dried precipitate was powdered (100 mesh) by grinding.

The catalysts containing various tungsten oxide contents were prepared by adding an aqueous solution of ammonium metatungstate $[(NH_4)_6(H_2W_{12}O_{40})\cdot nH_2O]$ (Aldrich) to the $Ti(OH)_4$ powder followed by drying and calcining at high temperatures for 4 h in air. This series of catalysts are denoted by their weight percentage of WO_3 and calcination temperature. For example, 10-WO_3/TiO_2 (500) indicates the catalyst containing 10 wt% WO_3 and calcined at 500 °C.

FTIR spectra were obtained in a heatable gas cell at room tem-

---

†To whom correspondence should be addressed.
E-mail: jrsohn@knu.ac.kr

This paper was presented at the 8th APCChE (Asia Pacific Confederation of Chemical Engineering) Congress held at Seoul between August 16 and 19, 1999.

perature by using a Mattson Model GL6030E spectrophotometer. The wafers contained about 9 mg/cm^2 self-supporting catalyst. Prior to obtaining the spectra the samples were heated under vacuum at 400-500 °C for 1.5 h.

The Raman spectra were obtained with a Spex Ramalog spectrometer with holographic gratings. The 5145-Å line from a Spectra-Physics Model 165 argon-ion laser was used as the exciting source. The laser beam was focussed onto an area 0.1×0.1 mm^2 in size of the sample surface; a 90° scattering geometry was used. The spectral shift width was typically 4 cm^{-1}, and laser source powers of approximately 45 mW, measured at the sample, were used.

X-ray photoelectron spectra was obtained with a VG scientific model ESCALAB MK-11 spectrometer. Al K_α and Mg K_α were used as the excitation source, usually at 12 kV, 20 mA. The analysis chamber was at 10^{-9} torr or better and the spectra of sample, as fine powder, were analyzed. Binding energies were referenced to the C_{18} level of the carbon at 284.6 eV.

Catalysts were checked in order to determine the structure of the support as well as that of tungsten oxide by means of a Jeol Model JDX-8030 diffractometer, employing Ni-filtered Cu K_α radiation.

DSC measurements were performed by a PL-STA model 1500H apparatus in air, and the heating rate was 5 °C per minute. For each experiment 10-15 mg of sample was used.

The acid strength of catalyst was measured qualitatively by using a series of the Hammett indicators [Sohn et al., 1996; Sohn and Park, 1998]. The catalyst in a glass tube was pretreated at 400 °C for 1 hr and filled with dry nitorgen. For the determination of acid strength of the catalyst the color changes of indicators were observed by spot test. Chemisorption of ammonia was employed as a measure of acidity of catalysts. The amount of chemisorption was obtained as the irreversible adsorption of ammonia [Sohn and Ozaki, 1980; Sohn and Ryu, 1993]. Thus the first adsorption of ammonia at 20 °C and 300 torr was followed by evacuation at 230 °C for 1 hr and readsorption at 20 °C, the difference between two adsorptions at 20 °C giving the amount of chemisorption. The specific surface area was determined by applying the BET method to the adsorption of nitrogen at −196 °C.

2-propanol dehydration was carried at 160 and 180 °C in a pulse micro-reactor connected to a gas chromatograph. Fresh catalyst in the reactor made of 1/4 inch stainless steel was pretreated at 400 °C for 1 h in the nitrogen atmosphere. Diethyleneglycol succinate on Simalite was used as packing material of the gas chromatograph and the column temperature was 180 °C for analyzing the product. Catalytic activity for 2-propanol dehydration was represented as mole of propylene converted from 2-propanol per gram of catalyst. Cumene dealkylation was carried out at 400-450 °C in the same reactor as above. Packing material for the gas chromatograph was Benton 34 on chromosorb W and column temperature was 130 °C. Catalytic activity for cumene dealkylation was represented as mole of benzene converted from cumene per gram of catalyst. Conversion for both reactions was taken as the average of the first to sixth pulse values.

RESULTS AND DISCUSSION

1. Raman and Infrared Spectra

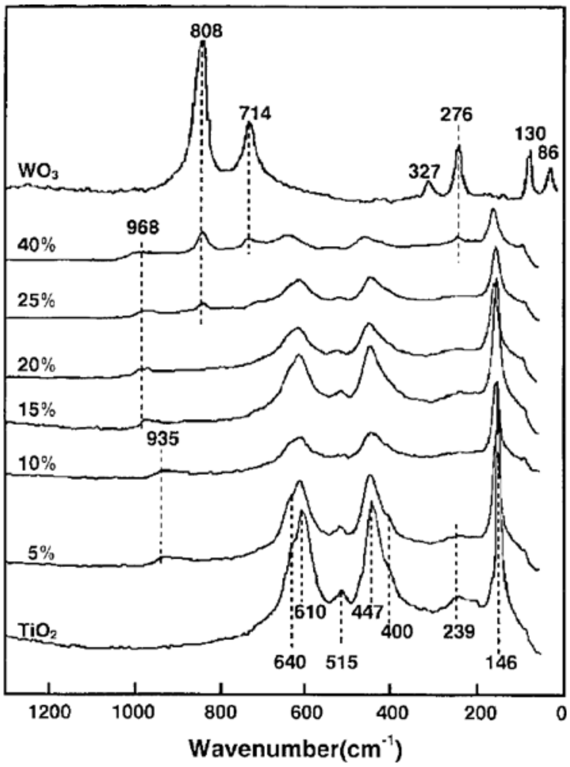

Fig. 1. Raman spectra of WO_3, WO_3/TiO_2 (450), and TiO_2.

The Raman spectra of WO_3 obtained by calcining ammonium metatungstate at 450 °C, WO_3/TiO_2 (450), and TiO_2 under ambient conditions are presented in Fig. 1. The WO_3 structure is made up of distorted WO_3 octahedra. The major vibrational modes of WO_3 are located at 810, 714, and 276 cm^{-1}, and have been assigned to the W=O stretching mode, the W=O bending mode, and the W-O-W deformation mode, respectively [Chan et al., 1984]. The Raman spectra of the WO_3/TiO_2 (450) samples at loading above 10% shows a weak and broad band at ~968 cm^{-1} which is characteristic of octahedrally coordinated polytungstate species [Vuurman et al., 1991]. The Raman spectra of the WO_3/TiO_2 samples containing 5 and 10 wt% of WO_3 show a weak and broad bands at ~935 cm^{-1} which is characteristic of tetrahedrally coordinated surface tungsten oxide species [Vuurman et al., 1991]. This assignment is in agreement with the $WO_3/\gamma\text{-}Al_2O_3$ system, where combined Raman and XANES data revealed the presence of distorted tetrahedral coordination at low loading [Horsley et al., 1987]. In addition to this 968 cm^{-1} band, the feature of titania at 640, 610, 515, 447, 400, 239, and 146 cm^{-1} is also present. The Raman spectrum of rutile TiO_2 is characterized by the bands at 610, 447, and 239 cm^{-1}, whereas the Raman band, with frequencies of 640, 515, 400, and 146 cm^{-1}, has been assigned to the anatase modification [Engweiler et al., 1996]. Therefore, TiO_2 sample calcined at 450 °C consists of a mixture of rutile and anatase phases, which is in agreement with the results of XRD described later.

The molecular structures of the supported tungsten oxide species depend on the loading. At loading above 20% three bands appear in the Raman spectrum at 808, 711, and 276 cm^{-1}, showing the presence of crystalline WO_3 [Chan et al., 1984]. These results are in good agreement with those of XRD described later. For 15-WO_3/TiO_2 sample the crystalline WO_3 phase was not observed, while for 30-WO_3/TiO_2 sample the triclinic phase of crystalline WO_3 appeared at the calcination temperature of 500-800 °C. Namely, below monolayer coverage such as 15-WO_3/TiO_2 only the surface tungsten oxide species exist on the TiO_2 surface due to the interaction between WO_3 and TiO_2. It seems likely that for 30-WO_3/TiO_2, monolayer coverage has been exceeded and WO_3 crystals are also present on the TiO_2 surface.

The Raman spectra above were recorded under ambient conditions. To examine the structure of tugnsten oxide complex under dehydration conditions, IR spectra of WO_3/TiO_2 samples were obtained in a heatable gas cell after evacuation at different temperatures for 1 h. The in situ IR spectra for 25-WO_3/TiO_2 (500) are presented for the range 1,100-900 cm^{-1} in Fig. 2. The IR single band at 1,003-1,012 cm^{-1} is due to the symmetrical W=O stretching mode of the tungsten oxide complex bonded to the TiO_2 surface. As evacuation temperature increases, the W=O stretching mode shifts upward from 1,003 to 1,012 cm^{-1}, the band shape becomes sharper, and the intensity increases. Similar results have been obtained with the other samples. This shows that dehydration changes the molecular structures and that the two-dimensional tetrahedrally coordinated tungsten oxide species as well as the octahedrally coordinated polytungstate species are converted into the same highly distorted, octahedrally coordinated structure as proposed by Wachs et al. [Vuurman et al., 1991]. The 1,012 cm^{-1} IR band matches the Raman absorption at 1,015 cm^{-1} [Vuurman et al., 1991]. However, the band at 1,015 cm^{-1} in Fig. 1 was not observed, because Raman spectra were recorded under ambient conditions.

2. X-ray Diffraction Patterns

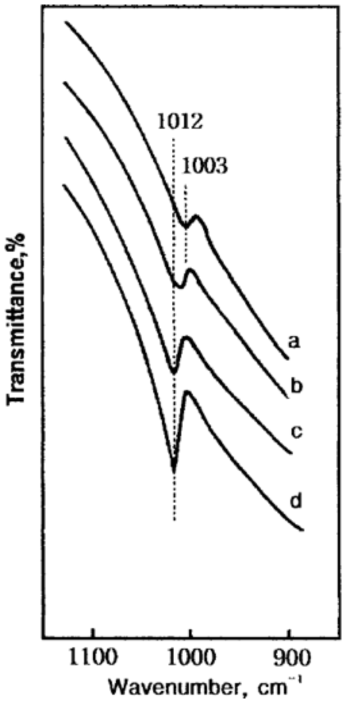

Fig. 2. IR spectra of 25-WO_3/TiO_2 (500) evacuated at different temperatures: (a) 25 °C, (b) 200 °C, (c) 300 °C, and (d) 400 °C.

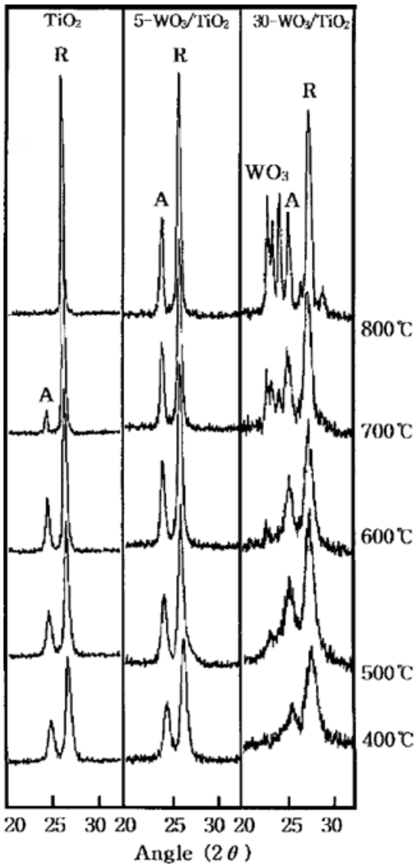

Fig. 3. X-ray diffraction patterns of TiO_2, 5-WO_3/TiO_2, and 30-WO_3/TiO_2 calcined at different temperatures for 4 h: A, anatase form TiO_2; R, rutile form TiO_2.

The crystalline structures of WO_3/TiO_2 calcined in air at different temperatures for 4 h were examined. As shown in Fig. 3, for pure TiO_2 X-ray diffraction data indicated a two-phase mixture of the rutile and anatase forms at 400-700 °C, and a rutile phase at 800 °C. However, in the case of supported tungsten oxide catalysts the crystalline structures of samples were different from that of the TiO_2 support. For the 5-WO_3/TiO_2, TiO_2 was present as a two-phase mixture of rutile and anatase forms at 400-800 °C. For pure TiO_2 only rutile form was observed at 800 °C. It is assumed that the interaction between tungsten oxide and TiO_2 hinders the transition of TiO_2 from anatase to rutile phase. The presence of tungsten oxide strongly influences the development of textural properties with temperature. No phase of tungsten oxide was observed up to 20 wt% at 500 °C, indicating a good dispersion of tungsten oxide on the surface of TiO_2 support due to the interaction between them. However, as shown in Fig. 3, for the 30-WO_3/TiO_2 the triclinic phase of crystaline WO_3 (2θ= 21.1, 23.6, and 24.4) due to the decomposition of ammonium metatungstate was observed in the samples calcined at 500-800 °C. These results are in good agreement with those of Raman spectra described above.

3. X-ray Photoelectron Spectra

Interactions with a support can dramatically change the properties of metals or metal oxides [Sohn et al., 1996]. Fig. 4 shows the W 4f spectra of WO_3/TiO_2 samples containing different tung-

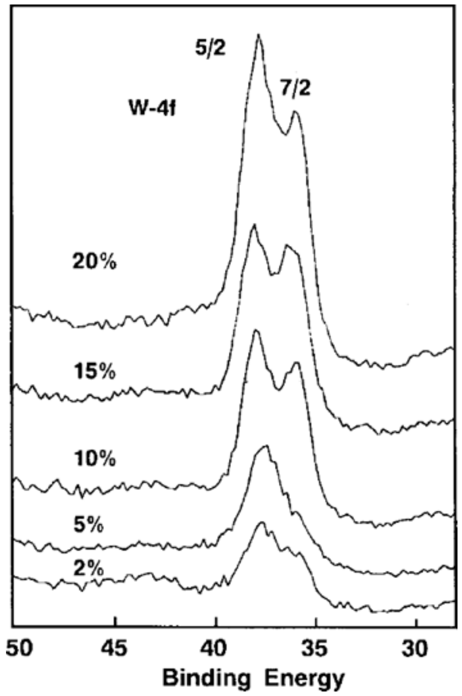

Fig. 4. W_{4f} XPS of WO_3/TiO_2 (500) having various WO_3 contents.

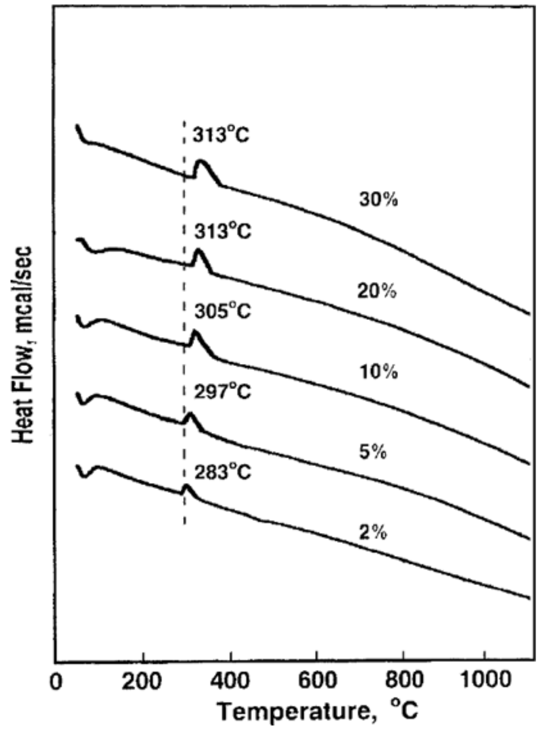

Fig. 5. DSC curves of precursors of WO_3/TiO_2 catalysts having various WO_3 contents.

Table 1. Specific surface area and acidity of WO_3/TiO_2 catalysts calcined at 500 °C for 4 h

Catalyst	Surface area (m^2/g)	Acidity (μmol/g)
TiO_2	52.1	68
2-WO_3/TiO_2	65.7	80
5-WO_3/TiO_2	69.7	86
10-WO_3/TiO_2	81.2	118
15-WO_3/TiO_2	90.5	144
20-WO_3/TiO_2	96.6	158
25-WO_3/TiO_2	94.1	124
30-WO_3/TiO_2	92.7	108
40-WO_3/TiO_2	81.8	100

sten oxide contents and calcined at 500 °C. The W 4f$_{7/2}$ binding energy measured for WO_3/TiO_2 samples occurred at 36 eV and corresponds to tungsten in the +6 oxidation state (WO_3) [Wachs et al., 1985]. Generally, the spectrum of supported WO_3 is broader than that of WO_3 due to the interaction between the WO_3 and support. It is known that there is a very strong interaction between WO_3 and Al_2O_3 so that tungsten oxide species are present as W^{+6} after calcination of WO_3/Al_2O_3 sample. As shown in Fig. 4, for WO_3/TiO_2 samples calcined in air tungsten oxide species are present as W^{+6}, indicating the strong interaction between WO_3 and TiO_2.

4. Thermal Analysis

In X-ray diffraction pattern, it was shown that the structure of WO_3/TiO_2 was different depending on the calcined temperature. To examine the thermal properties for the precursors of samples more clearly, their thermal analysis was carried out. For pure TiO_2 the DSC curve showed a broad endothermic peak below 180 °C due to water elimination, and an exothermic peak at 280 °C due to the TiO_2 crystallization. In the case of WO_3/TiO_2 two additional endothermic peaks appeared at 50 °C and 300 °C due to the revolution of NH_3 and H_2O decomposed from ammonium metatungstate. However, it is of interest to see the influence of WO_3 on the crystallization of TiO_2 from amorphous to anatase phase. As shown in Fig. 5, the exothemic peak due to the crystallization of TiO_2 appeared at 280 °C for pure TiO_2, while for WO_3/TiO_2 it was shifted to higher temperatures. The shift increased with increasing WO_3 content. It is considered that the interaction between WO_3 and TiO_2 delays the transition of TiO_2 from amorphous to anatase phase [Sohn et al., 1996].

5. Surface Properties

It is necessary to examine the effect of tungsten oxide on the surface properties of catalysts, that is, specific surface area, acidity, and acid strength. The specific surface areas of samples calcined at 500 °C for 4 h are listed in Table 1. The presence of tungsten oxide strongly influences the surface area in comparison with the pure TiO_2. Specific surface areas of WO_3/TiO_2 samples are much larger than that of pure TiO_2 calcined at the same temperature, showing that surface area increases gradually with increasing tungsten oxide content up to 20 wt% of WO_3. It seems likely that the interaction between tungsten oxide and TiO_2 protects catalysts from sintering.

The acid strength of the catalysts was examined by a color change method, using Hammett indicator in sulphuryl chloride. The results are listed in Table 2. In this table, (+) indicates that the color of the base form was changed to that of the conjugated acid form. TiO_2 evacuated at 400 °C for 1 h has an acid stength $H_0 \leq +1.5$, while 5-WO_3/TiO_2 and 15-WO_3/TiO_2 were estimated to have a $H_0 \leq -14.5$, indicating the formation of new acid sites

Table 2. Acid strengths of some samples

Hammett indicator	pKa	TiO_2	5-WO_3/ TiO_2 (500)	15-WO_3/ TiO_2 (500)
Benzeneazodiphenylamine	+1.5	+	+	+
Dicinnamalacetone	−3.0	-	+	+
Benzalacetophenone	−5.6	-	+	+
Anthraquinone	−8.2	-	+	+
Nitrobenzene	−12.4	-	+	+
2, 4-dinitrofluorobenzene	−14.5	-	+	+

stronger than those of single oxide components. Acids stronger than $H_0 \leq -11.93$, which corresponds to the acid stength of 100% H_2SO_4, are superacids [Sohn and Park, 1998]. Consequently, WO_3 /TiO_2 catalysts would be solid superacids. The superacidic property is attributed to the double bond nature of the W=O in the complex formed by the interaction of TiO_2 with tungstate, in analogy with the case of ZrO_2 modified with chromate and sulfate ion [Sohn and Ryu, 1993].

The acidity of catalysts calcined at 500 °C, as determined by the amount of NH_3 irreversibly adsorbed at 230 °C [Sohn and Ryu, 1993; Sohn et al., 1996], is listed in Table 1. As listed in Table 1, the acidity increases upon the addition of 2 wt% tungsten oxide to TiO_2, and then the acidity increases very gently with increasing tungsten oxide content up to 20 wt% of WO_3. It is clear that the acidity is correlated with the specific surface area. Many combinations of two oxides have been reported to generate acid sites on the surface [Tanabe et al., 1989]. The combination of TiO_2 and WO_3 probably generates stronger acid sites and more acidity as compared with the separate components.

Infrared spectroscopic studies of ammonia adsorbed on solid surface have made it possible to distinguish between Brönsted and Lewis acid sites [Satsuma et al., 1988]. Fig. 6 shows the IR spectra of ammonia adsorbed on 30-WO_3/TiO_2 (500) calcined and evacuated at 400 °C for 1 h. For 30-WO_3/TiO_2 (500) the bands at 1,428 are the characteristic peaks of ammonium ion, which are formed on the Brönsted acid sites and the other set of adsorption peaks at 1,620 cm^{-1} is contributed by ammonia coordinately bonded to Lewis acid sites [Satsuma et al., 1988], indicating the presence of both Brönsted and Lewis acid sites. Other samples having different WO_3 content also showed the presence of both Lewis and Brönsted acid sites. Therefore, these WO_3/TiO_2 samples can be used as catalysts for Lewis or Brönsted acid catalysis.

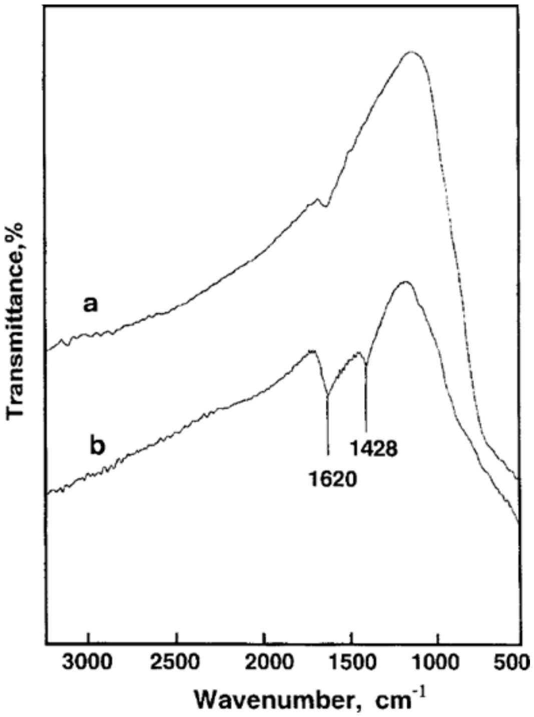

Fig. 6. Infrared spectra of NH_3 adsorbed on 30-WO_3/TiO_2 (500) : (a) background of 30-WO_3/TiO_2 (500) and (b) NH_3 adsorbed on 30-WO_3/TiO_2 (500). Gas phase was evacuated at 230 °C for 1 h after adsorption.

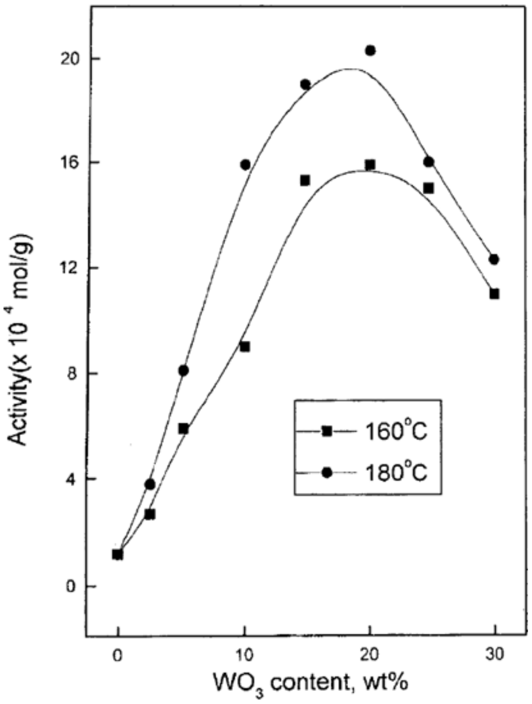

Fig. 7. Catalytic activities of WO_3/TiO_2 (500) for 2-propanol dehydration as a function of WO_3 content.

6. Catalytic Activities for Acid Catalysis

It is interesting to examine how the catalytic activity of acid catalyst depends on the acidic property. For both reactions WO_3/ TiO_2 catalysts calcined at 450-500 °C exhibited the highest catalytic activities. The catalytic activities for the 2-propanol dehydration and cumene dealkylation are measured and the results are illustrated as a function of WO_3 content in Figs. 7 and 8, respectively, where reaction temperatures are 160-180 °C for 2-propanol dehydration and 400-450 °C for cumene dealkylation. In view of Table 1 and Figs. 7 and 8, the variation in catalytic activity for 2-propanol dehydration is correlated with the change of acidity. However, the variation in catalytic activity for cumene dealkylation is roughly correlated with that of acidity. The differences of catalytic activities for both reactions against acidity are due to the difference of necessary acid strength for both reactions to occur. In fact, it has been known that 2-propanol dehydration takes place very readily on weak acid sites, while cumene

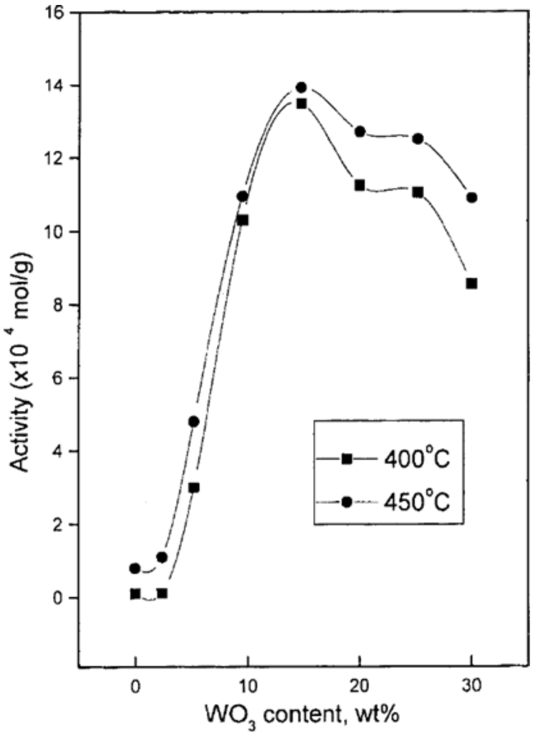

Fig. 8. Catalytic activities of WO_3/TiO_2 (500) for cumene dealkylation as a function of WO_3 content.

dealkylation does on relatively strong acid sites [DeCanio et al., 1986]. In view of the catalytic data shown in Figs. 7 and 8 for 2-propanol dehydration and cumene dealkylation reactions, where the reaction temperatures were 160-180 °C for the former and 400-450 °C for the latter, it is clear that 2-propanol dehydration takes place more readily than cumene dealkylation.

CONCLUSIONS

This paper has shown that a combination of FTIR, Raman spectroscopy, and XRD can be used to perform the characterization of WO_3/TiO_2 prepared by drying a mixed solution of ammonium metatungstate and $Ti(OH)_4$ and calcining in air. The interaction between tungsten oxide and titania influences the physicochemical properties of prepared catalysts with calcination temperature. The specific surface area and acidity of catalysts increase in proportion to the tungsten oxide content up to 20 wt%. Since the TiO_2 stabilizes the surface tungsten oxide species, for the samples equal to or less than 20 wt%, tungsten oxide was well dispersed on the surface of titania, but for the samples above 20 wt% the triclinic phase of WO_3 was observed at any calcination temperature. Upon the addition of only a small amount of tungsten oxide (2 wt%) to titania, both the acidity and acid strength of the catalyst increases remarkably, showing the presence of Brönsted and Lewis acid sites on the surface of WO_3/TiO_2. The high acid strength and high acidity are responsible for the W=O bond nature of complex formed by the interaction between WO_3 and TiO_2. The catalytic activities of WO_3/TiO_2 catalysts for 2-propanol dehydration and cumene dealkylation were roughly correlated to their acidity.

ACKNOWLEDGEMENT

This work was supported by the Korea Science and Engineering Foundation (Grant No.: 981-1101-004-2) and the Research Center for Catalytic Technology at Pohang University of Science and Technology.

REFERENCES

Adeeva, V., de Haan, J. W., Janchen, J., Lei, G. D., Schunemann, V., van de Ven, L. J. M., Sachtler, W. M. N. and van Santen, R. A., "Acid Sites in Sulfated and Metal-promoted Zirconium Dioxide Catalysts," *J. Catal.*, **151**, 364 (1995).

Alemany, L. J., Berti, F., Busca, G., Ramis, G., Robba, D., Toledo, G. P. and Trombetta, M., "Characterization and Composition of Commercial V_2O_5-WO_3-TiO_2 SCR Catalysts," *Appl. Catal. B: Enviromental*, **10**, 299 (1996).

Arata, K., "Solid Superacids," *Adv. Catal.*, **37**, 165 (1990).

Basrur, A. G., Parwardham, S. R. and Vyas, S. N., "Propene Metathesis over Silica-supported Tungsten Oxide Catalyst-catalyst Induction Mechanism," *J. Catal.*, **127**, 86 (1991).

Chan, S. S., Wachs, I. E. and Murrell, L. L., "Relative Raman Cross-sections of Tungsten Oxides," *J. Catal.*, **90**, 150 (1984).

Cheung, T. K., d'Itri, J. L., Lange, F. C. and Gates, B. C., "Neopentane Cracking Catalyzed by Iron and Manganese-promoted Sulfated Zirconia," *Catal. Lett.*, **31**, 153 (1995).

DeCanio S. J., Sohn, J. R., Fritz, P. O. and Lunsford, J. H., "Acid Catalysis by Dealuminated Zeolite-Y," *J. Catal.*, **101**, 132 (1986).

Ebitani, K., Konish, J. and Hattori, H., "Skeletal Isomerization of Hydrocarbons over Zirconium Oxide Promoted by Platinum and Sulfatelion," *J. Catal.*, **130**, 257 (1991).

Engweiler, J., Harf, J. and Baiker, A., "WO_x/TiO_2 Catalysts Prepared by Grafting of Tungsten Alkoxides: Morphological Properties and Catalytic Behavior in the Selective Reduction of NO by NH_3," *J. Catal.*, **159**, 259 (1996).

Figueras, F., Coq, B., Walter, C. and Carriat, J. Y., "Hydroconversion of Methylcyclohexane on Bifunctional Sulfated Zirconia-supported Platinum Catalysts," *J. Catal.*, **169**, 103 (1997).

Guitierrez-Alejandre, A., Ramirez, J. and Busca, G., "A Vibrational and Spectroscopic Study of WO_3/TiO_2-Al_2O_3 Catalyst Precursors," *Langmuir*, **14**, 630 (1998).

Hino, M. and Arata, K., "Synthesis of Solid Superacid of Tungsten Oxide Supported on Zirconia and its Catalytic Action for Reactions of Butane and Pentane," *J. Chem. Soc., Chem. Commun.*, 1259 (1988).

Horsley, J. A., Wachs, I. E., Brown, J. M., Via, G. H. and Hardcastle, F. D., "Structure of Surface Tungsten Oxide Species in the WO_3/Al_2O_3 Supported Oxide System from X-ray Absorption Near-edge Spectroscopy and Raman Spectroscopy," *J. Phys. Chem.*, **91**, 4014 (1987).

Hsu, C. Y., Heimbuch, C. R., Armes, C. T. and Gates B. C., "A Highly Active Solid Superacid Catalyst for n-Butane Isomerization: a Sulfated Oxide Containing Iron, Manganese and Zirconium," *J. Chem. Soc., Chem. Commun.*, 1645 (1992).

Keogh, R. A., Srinivasan, R. and Davis, B. H., "Pt-SO_4^{2-}-ZrO_2 Catalysts the Impact of Water on Their Activity for Hydrocarbon Conversion," *J. Catal.*, **151**, 292 (1995).

Lee, J. K. and Rhee, H. K., "Effect of Metal/Acid Balance in Pt-loaded Large Pore Zeolites on the Hydroisomerization of n-Hexane and n-Heptane," *Korean J. Chem. Eng.*, **14**, 451 (1997).

Meijers, S., Gielgens, L. H. and Ponec, V., "IR Spectroscopic Study of the Skeletal Isomerization of Butane by Alumina-supported Tungsten Oxide Catalysts," *J. Catal.*, **156**, 147 (1995).

Satsuma, A., Hattori, A., Mizutani, K., Furuta, A., Niyamoto, A., Hattori, T. and Murakami, Y., "Surface Active Sites of V_2O_5-WO_3 Catalysts," *J. Phys. Chem.*, **92**, 6052 (1988).

Sohn, J. R., Cho, S. G., Pae, Y. I. and Hayashi, S., "Characterization of Vanadium Oxide-zirconia Catalyst," *J. Catal.*, **159**, 170 (1996).

Sohn, J. R., Jang, H. J. and Kim, H. W., "Catalytic Activities and Acid Strengths of NiO-ZrO_2 Catalysts Modified with Acids," *Korean J. Chem. Eng.*, **7**, 7 (1990).

Sohn, J. R. and Ozaki, A., "Acidity of Nickel Silicate and its Bearing on the Catalytic Activity for Ethylene Dimerization and Butene Isomeriation," *J. Catal.*, **61**, 29 (1980).

Sohn, J. R. and Park, M. Y., "Characterization of Zirconia-supported Tungsten Oxide Catalyst," *Langmuir*, **14**, 6140 (1998).

Sohn, J. R. and Ryu, S. G., "Surface Characterization of Chromium Oxide-zirconia Catalyst," *Langmuir*, **9**, 126 (1993).

Tanabe, K., Misono, M., Ono, Y. and Hattori, J., "New Solid Acids and Bases," Elsevier Science, Amsterdam (1989).

Vaudagna, S. R., Conelli, R. A., Canavese, S. A. and Figoli, N. S., "SO_4^{2-}-ZrO_2 and Pt/SO_4^{2-}-ZrO_2: Activity and Stability during n-Hexane Isomerization," *J. Catal.*, **169**, 389 (1997).

Vuurman, M. A., Wachs, I. E. and Hirt, A. M., "Structural Determination of Supported V_2O_5-WO_3/TiO_2 Catalysts by in situ Raman Spectroscopy and X-ray Photoelectron Spectroscopy," *J. Phys. Chem.*, **95**, 9928 (1991).

Wachs, I. E., Chersich, C. C. and Hardenbergh, J. H., "Reduction of WO_3/Al_2O_3 and Unsupported WO_3 : A Comparative ESCA Study," *Appl. Catal.*, **13**, 335 (1985).